International Journal of Mass Spectrometry 280 (2009) 50–56

Contents lists available at ScienceDirect

International Journal of Mass Spectrometry

journal homepage: www.elsevier.com/locate/ijms

On the development of an effective model potential to describe water interaction in neutral and ionic clusters

M. Albertí[a], A. Aguilar[a], D. Cappelletti[b], A. Laganà[b,*], F. Pirani[b]

[a] IQTCUB, Dept. de Química Física, Universitat de Barcelona, Barcelona, Spain
[b] Università di Perugia, Perugia, Italy

ARTICLE INFO

Article history:
Received 20 May 2008
Received in revised form 10 July 2008
Accepted 18 July 2008
Available online 30 July 2008

This paper is dedicated to Zdenek Herman a good friend and a dedicated scientist who has carried out research relevant to the study of ionic aggregates (see for instance [J. Jašik, J. Roithová, J. Žabka, R. Thissen, I. Ipolyi, Z. Herman, I.J. Mass. Spec. 255–256 (2006) 150]).

Keywords:
Van der Waals
Water interaction
Small clusters

ABSTRACT

Various effective components of the intermolecular interaction of water containing aggregates are examined and their modeling, in terms of the fundamental physical properties of the involved partners, is discussed. We focus, in particular, on the evolution of these components in going from the simplest neutral rare gas–water aggregates to bulk water and ionic water solutions. The analysis singled out that the model chosen to represent the van der Waals interaction as the composition of the action of three dispersion/induction–attraction centres and found to be appropriate to describe the lighter He–H_2O and Ne–H_2O systems, is not adequate to describe the heavier Ar–H_2O aggregate. It was found, instead, that by increasing the mass of the rare gas, other short range contributions to the interaction come into play. Moreover, it was also found that the water molecule tends to behave as a single centre as the strength of the interaction increases. This led to the development of an effective model potential suitable to describe water clusters in the range going from gaseous to condensed phase. The role of electrostatic contributions is also evaluated. The proposed potential model is tested by comparing molecular beam scattering and neutron diffraction experiments with results of molecular dynamics (MD) calculations.

1. Introduction

Characterization and modeling of the different components of the intermolecular interaction in molecular aggregates involving water molecules, is of crucial importance in describing static and dynamic properties of several chemical systems and processes, both in condensed (solid and solution) and in gas phase, as well as in neutral and ionic situations. In general, following the usual force field approach, the intermolecular interaction is described in terms of non-covalent (like size-repulsion, dispersion/induction–attraction and electrostatic effects) and chemical (like charge transfer) components [1,2]. The relative importance of these components, because of their weakness and their incomplete separability, still remains to a large extent to be understood, especially when systems of increasing complexity are considered. In the specific case of water, the balancing of the various components is particularly difficult because the molecular outer electronic charge distribution varies significantly in going from gas (isolated molecules) to condensed (interacting molecules) phase [3–5].

Clusters spectroscopy (see for instance Ref. [6]), scattering cross-sections and second virial coefficients in gas phase [7–13], and neutron diffraction [14–16] in condensed phase, have been used as experimental probes of the water interaction.

Various empirical potential models have already been proposed in the literature though most of the related formulations bear limited validity and satisfactorily reproduce only some of the water properties [4,5]. This is attributable both to the different formulation of the electrostatic term (which dominates, when present, the long range interaction) and to an inaccurate representation of the size-repulsion and dispersion–attraction components (globally known as van der Waals) of the interaction. An accurate description of the van der Waals component is vital to develop a unified view of the water interaction and a sufficiently general effective model potential. As a matter of fact, while dispersion usually accounts only for a small fraction of the total interaction energy, size-repulsion plays a more crucial role since it determines the equilibrium distance of the building blocks in a polyatomic aggregate.

This problem was brought to attention by recent scattering experiments [10,11], which evidenced the coming into play of

* Corresponding author at: Dipartimento di Chimica, Università di Perugia, Via Elce di Sotto, 8, Perugia 06123, Italy.
E-mail address: lag@dyn.unipg.it (A. Laganà).

1387-3806/$ – see front matter © 2008 Elsevier B.V. All rights reserved.
doi:10.1016/j.ijms.2008.07.018

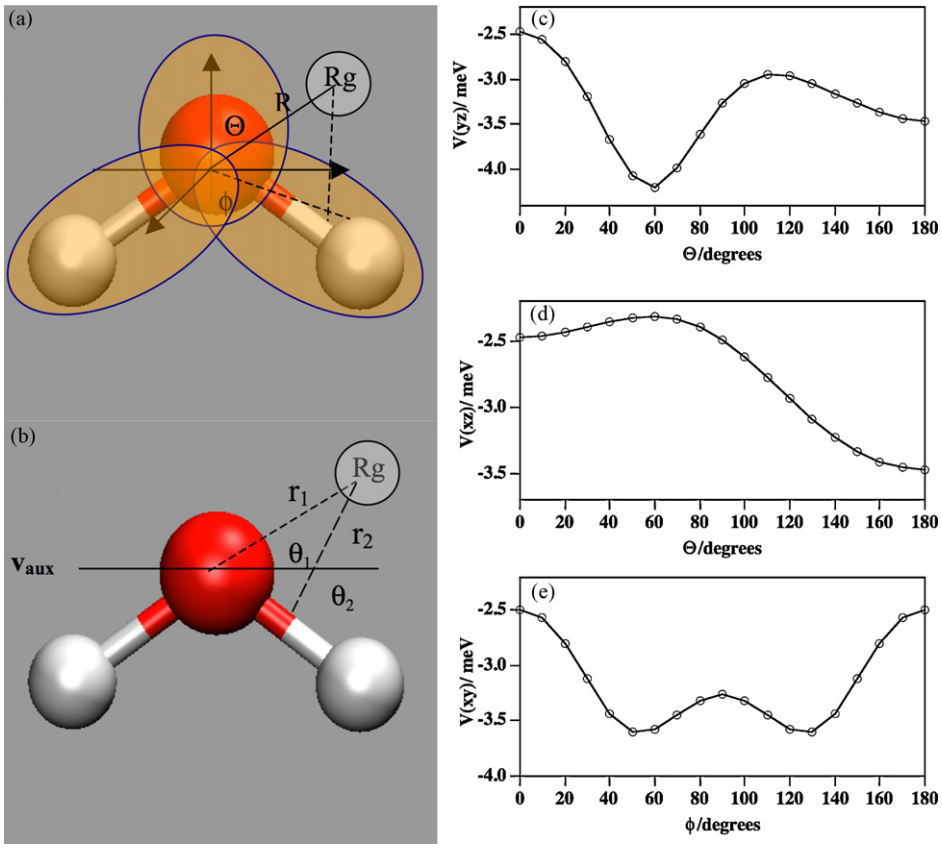

Fig. 1. Left-hand side panels: (a) schematic representation of the polarizability ellipsoids of H_2O and polar coordinates; (b) sketch of the variables used to define V_{vdW} (see text). Right-hand side panels: minimum interaction energy of the He–H_2O system plotted as a function of θ when He moves (c) on the molecular plane ($\phi = 90$); (d) on the perpendicular plane bisecting the HOH angle ($\phi = 0$) and as a function of ϕ when (e) He moves on a perpendicular plane containing $\mathbf{v}_{aux}$ ($\theta = 90$).

a component additional to the van der Waals interaction when moving from He–H_2O to Xe–H_2O. This prompted the need for properly representing the size-repulsion and dispersion–attraction by first rationalizing the behavior of systems like the rare gas–water clusters (Rg–H_2O) in which these two terms are the leading components of the interaction. Among them, He–H_2O and Ne–H_2O are the most instructive cases, because related interactions depend only on the two mentioned components (plus a weak induction associated with the permanent dipole-induced dipole effect). The investigation of the heavier Rg–H_2O systems singled out, instead, the coming into play of additional short range contributions [11]. In this context, we believe that a comparative study of Rg–H_2O aggregates as a function of the mass (and accordingly of the strength of the interaction) helps in understanding the role of the van der Waals component for systems containing water and provides information on the parameters to be used for its description when the strength of the interaction increases.

The present paper starts in Section 2 by defining the interaction components involved in the model and by representing the water polarizability, a basic physical property affecting both attraction and repulsion (see for instance Refs. [11] and [17]), as a combination of three components with axial symmetry (the so-called molecular polarizability ellipsoids [18,19]). It is then emphasized that the position of the centres of such ellipsoids (also called dispersion/induction centres) tends to converge into a single centre placed on the oxygen atom as the strength of the interaction increases and a more general formulation of the potential is given. The model is then extended in Section 3 to the analysis of larger $(H_2O)_n$ clusters, liquid water and M^+–H_2O (M^+: alkali ion) ionic solutions and a comparison of the results of some molecular dynamics (MD) simulations with the experimental data is given.

2. The proposed polarizability based effective model intermolecular potential

In order to meet the portability needs of MD computations, the intermolecular potential V is often expressed as a combination of few effective terms, defined by a limited number of parameters related to basic physical properties of the interacting partners [20–26]. Therefore, following the guidelines given in Refs. [1,25], the potential V is represented as a combination of size-repulsion (V_{rep}), dispersion (V_{disp}) and induction (V_{ind}) attraction, electrostatic (V_{electr}) and charge transfer (V_{ctr}) effective contributions,

$$V = V_{rep} + V_{disp} + V_{ind} + V_{electr} + V_{ctr} \quad (1)$$

The various contributions need to be considered as effective components due to their incomplete separability, especially when the intermolecular distance becomes small.

The model assumes that the isolated water molecule can be described as a combination of three polarizability ellipsoids like those shown in Fig. 1 a, of which two refer to the OH bonds and the third refers to the electronic cloud (including the lone pairs) located around the O atom. This choice, which can be understood in terms of the related HOMO orbitals, proceeds from the basic features of the electronic structure of H_2O [3]. At the same time, the weak van der Waals interaction ($V_{vdW} = V_{rep} + V_{disp}$) between a closed shell atom and a water molecule can be represented as a sum of the contributions associated with the three atom-polarizability ellipsoid pairs, equivalent to three atom-bond terms [27](see next

subsection for further details). In order to account for the modifications that the electronic structure of water can undergo under the effect of the intermolecular field, the hardness of the repulsive wall and the position of the dispersion/induction centres along the OH bonds (and, accordingly, their influence on the global intermolecular interaction) are allowed to vary for different aggregates while, as usual, the water molecule is assumed to be rigid.

2.1. The Rg–H_2O aggregates (Rg= He, Ne, Ar)

As already mentioned, our work has focused at its beginning on the Rg–H_2O systems, which are the aggregates involving the minimum number of interaction components since, for these systems, V_{electr} is absent and V_{ind} plays a minor role. This situation is ideal to carry out an almost *in vitro* analysis of V_{vdW} and to relate it to the position of the molecular polarizability ellipsoid centres. For this reason we applied the model to the formulation of the weak interaction of the He–H_2O and Ne–H_2O, taken as reference systems, for which V can be expressed as a sum of three potentials, $V_i(r,\theta)$ of the V_{vdW} type, plus the term V_{ind}, arising from the permanent dipole of water,

$$V = \sum_{i=1}^{3} V_i(r,\theta) + V_{ind} \tag{2}$$

For the Rg— OH interaction r is the distance of Rg from the centre of the polarizability ellipsoid, relevant to the definition of the dispersion centre placed along the OH bond. At the same time θ is the angle formed by **r** and the OH bond (both these r and θ are labeled by index 2 in Fig. 1b).

For Rg— O the potential is formulated using an auxiliary vector $\mathbf{v}_{aux}$ (parallel to the HH internuclear distance and placed on the O atom). For this pair, r is the distance between Rg and O and θ is the angle formed by **r** and $\mathbf{v}_{aux}$ (both these r and θ are labeled by index 1 in Fig. 1b).

All the $V_i(r,\theta)$ terms of Eq. (2) are formulated as

$$V_i(r,\theta) = \varepsilon(\theta)\left[\frac{m}{n(r,\theta)-m}\left(\frac{r_0(\theta)}{r}\right)^{n(r,\theta)} - \frac{n(r,\theta)}{n(r,\theta)-m}\left(\frac{r_0(\theta)}{r}\right)^{m}\right] \tag{3}$$

where the positive lhs contribution describes the repulsion, while the negative rhs one, with $m = 6$, describes the dispersion–attraction interaction. The ε and r_0 pair of parameters, defining the well depth and its location, respectively, are expressed as a weighted sum of parallel ($\varepsilon_\parallel$ and $r_{0\parallel}$) and perpendicular ($\varepsilon_\perp$ and $r_{0\perp}$) contributions (see for details Refs. [26,27]). It is important to emphasize here that the exponent of the repulsive part of the interaction in Eq. (3), varies with r and depends on r_0 and β as follows,

$$n(r,\theta) = \beta + 4.0\left(\frac{r}{r_0(\theta)}\right)^2 \tag{4}$$

Note that β is an adjustable parameter modulating the hardness of the repulsion and r/r_0 is a scaled distance parameter controlling the dependence of both the repulsive and the attractive term on r at the various values of θ. Such dependences remove most of the inadequacies of the Lennard Jones (LJ) model potential [28,29] still widely used in molecular dynamics simulations. The values of ε and r_0 can be estimated from atomic and molecular polarizabilities [26]. The induction, which accounts only for a few percent of the global attraction, is formulated, as suggested by its asymptotic expression [30], in terms of the water permanent dipole moment (1.85 D) and the rare gas polarizability.

Table 1
Potential parameters for the Rg–H_2O systems

Rg–X	$\varepsilon_\parallel$ (meV)	$r_{0\parallel}$ (Å)	$\varepsilon_\perp$ (meV)	$r_{0\perp}$ (Å)
He— OH	1.120	3.300	1.140	3.151
He— O	2.326	3.050	0.750	3.684
Ne— OH	2.060	3.394	1.997	3.267
Ne— O	4.228	3.167	1.510	3.760
Ar— OH	3.879	3.742	3.358	3.663
Ar— O	6.320	3.562	2.796	4.080

For the Rg–H_2O systems the interaction is weak. Because of this, the geometry of H_2O has been assumed to coincide with that of the isolated molecule in gas phase. Accordingly, the length of the OH bond has been set equal to 0.9572 Å and the width of the HOH angle equal to 104.52°.

To examine the influence on V of both the repulsive wall hardness and the dispersion centre position along the OH bonds, the β parameter has been initially taken equal to 9, its typical value for close-shell systems [28], and the dispersion centre has been initially placed on the middle point of the OH bond, as in previous studies [28,31–34]. The values used for the other parameters are listed in Table 1.

2.2. On the reliability of the proposed effective model potential for Rg–H_2O aggregates

The proposed effective model potential is able to describe the weak interaction for all the lighters Rg–H_2O aggregates without any significant variations in both the value of β and in the position of the dispersion centre on the OH ellipsoid. As a matter of fact, it has been found that, when using $\beta = 9$ and small displacements of the dispersion centre, placed at $0.55 \cdot r_{OH}$ from O for He–H_2O and at $0.48 \cdot r_{OH}$ for Ne–H_2O (r_{OH} is the OH equilibrium distance), the model provides potential energy surfaces (PESs) having characteristics similar to those given in the literature [7–13,35,36]. Table 2 reports data related to the equilibrium geometry of each system (R and V) and to the spherically averaged interaction (R_0, ε_0). For the sake of comparison, some features of the systems calculated on the adopted model potential (no best fit was made) are compared with recent *ab initio* data and molecular beam scattering experimental results.

Further details on the characteristics of the He–H_2O PES are illustrated in the right hand side of Fig. 1(panels c, d and e), where the variation of the interaction energy at the potential minimum with the angle is plotted for some specific He motions: panel (c) He moves on the plane containing the molecule, panel (d) He moves on the perpendicular plane bisecting the HOH angle, panel (e) He moves on the perpendicular plane containing $\mathbf{v}_{aux}$.

However, the direct comparison of calculated data with scattering measurements is a truly crucial test for judging the validity of a PES. In Ref. [37] the measured integral cross-sections for He–H_2O and Ne–H_2O [10,11] have been compared with the predictions of the

Table 2
Predicted intermolecular distance R (see Fig. 1a), interaction energy V and angle θ for the most stable configuration of the system considered

System	R (Å)	V (meV)	θ (degree)	R_0 (Å)	ε_0 (meV)
He–H_2O	3.23	−4.195	60	3.43	2.91
	3.14[a]	−4.193[a]	74[a]	3.45[b]	2.75[b]
Ne–H_2O	3.34	−7.646	61	3.49	5.56
	3.23[c]	−8.008[c]	76[c]	3.50[d]	5.70[d]

The well depth ε_0 and its location R_0 for the isotropic interaction, are also given together with *ab initio*[a,c] and scattering experiments[b,d] results. (a,c) Results of VB in Ref.[36] and of Ref. [13]; (b,d) Results from scattering experiments [10,11].

effective model potential presented here. It has been found that the theoretical results reproduce quite well the measured data.

For the heavier Rg–H_2O systems the analysis of the experimental data pointed out [11] that the interaction energy is larger than that expected from the van der Waals component corrected for induction effects. This indicates that the present model, which includes only V_{vdW} and V_{ind}, is unable to describe alone the interaction even for Ar–H_2O. On the contrary, an improvement is obtained by decreasing the size and the hardness of the repulsive wall, especially for some specific geometries of the aggregate. This effect is achieved by placing the dispersion centre of the OH ellipsoids at a distance of $0.1 \cdot r_{OH}$ from O and reducing at the same time the β value to 6.6. The persisting difference between the potential derived from the experiments and that obtained from the model, suggests that an attractive component, intervening at intermediate and short intermolecular distances, is still missing [11]. This is also confirmed by a comparison of the value of the energy minimum (−14.4 meV) predicted by the model with that obtained from *ab initio* calculations, whose estimates fall in the interval ranging from −16.7 to −17.8 meV [13]. Therefore, further work is needed to characterize the increase of the attraction (preliminarly assigned to a charge transfer contribution [11]) though its relative contribution to the overall potential tends to vanish when further interaction components (like V_{electr}), stronger than pure dispersion–attraction, come into play.

A key result of the analysis of the interaction of the Rg–H_2O systems is the observation that the locations of the dispersion centres, distributed over various points of the water molecular frame, tend to converge into a common point located on the oxygen atom, as the strength of the interaction increases.

2.3. From Rg–H_2O to $(H_2O)_n$ clusters ($n = 2$, 3 and 4)

As a next step we considered the extension of the effective model potential to the description of the water–water interaction, that is stronger than that of Rg–H_2O systems mainly because of the presence of V_{electr}. This pushed us to incorporate V_{ind} and V_{ctr} into more important effective components. The incorporation was achieved by displacing the dispersion centre on the OH bond and by increasing the dipole moment of the water monomer in the clusters defined through a three-point charge distribution. As usual, V_{electr} was formulated as a sum of Coulombic terms and the dipole moment of the monomer, μ, in the clusters was taken equal to 2.1, 2.21 and 2.26 D [38–40] for the dimer, trimer and tetramer, respectively. The effect of varying the position of the dispersion centre along the OH bond was investigated again in detail by calculating the dissociation energy as a function of the distance ($\mathbf{r}_O$) of the oxygen atom from the dispersion centre. These values are plotted as a solid circles in the upper, central and lower panel of Fig. 2. In the same panels the values of the dissociation energy of the dimer, the trimer and the tetramer obtained from recent *abinitio* calculations [6,41] are also reported as empty circles at $\mathbf{r}_O = 0$, for comparison. As is apparent from the figure the empty circle values look like an extrapolation of the solid circles ones.

These results indicate that a water molecule in water clusters is well represented in terms of a unique dispersion centre ($\bar{O}$) placed on the oxygen atom bearing the overall polarizability of the water molecule. This led to the development of a new effective model potential called Adapted Molecular Polarizability centres for Force fields (AMPF) [40] for water clusters in which V_{vdW} is calculated by removing the angular dependence in Eqs. (3) and (4). The AMPF model is therefore formulated as

$$V_{vdW}(R) = V_{\bar{O}\bar{O}} = \varepsilon \left[\frac{m}{n(R) - m} \left(\frac{R_0}{R} \right)^{n(R)} - \frac{n(R)}{n(R) - m} \left(\frac{R_0}{R} \right)^{m} \right] \quad (5)$$

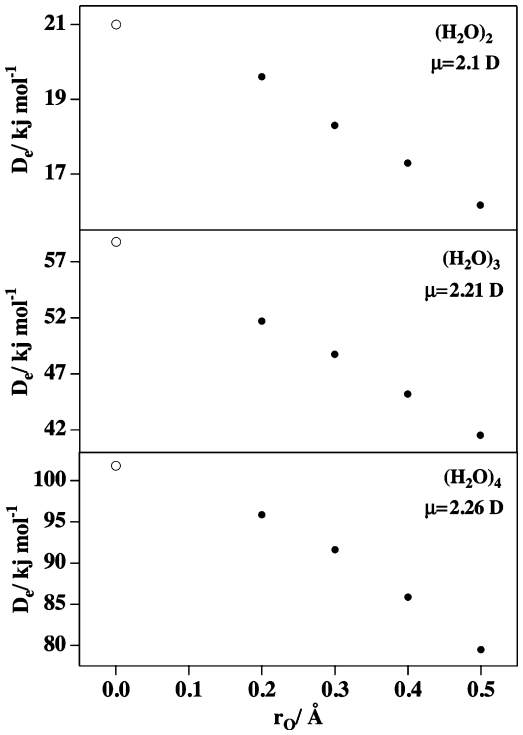

Fig. 2. Values of the predicted dissociation energy D_e (solid circles) for dimer (upper panel), trimer (medium panel) and tetramer (lower panel) plotted as a function of the distance $\mathbf{r}_O$ of the oxygen atom from the dispersion centre along the OH bond. For comparison, *a* b initio values [6,41] are shown as empty circles at $\mathbf{r}_O = 0$.

where $n(R) = \beta + 4.0(R/R_0)^2$ and R (having the meaning of the distance between the O atoms of the two water molecules considered) instead of r (the distance between the atom and the dispersion centre) is used.

The required parameter values ($\varepsilon = 9.06$ meV, $R_0 = 3.73$ Å) are estimated from the overall polarizability of the water molecule ($\alpha = 1.47$ Å^3) and to β is given the value of 6.6 that is lower than the usual one of 9 (see Section 2.1) to take into account the possibility of forming hydrogen bonds.

The AMPF model potential ensures a good estimate of the equilibrium energy and geometry of the small clusters [6,41–45]. For instance, Fanourgakis and Xantheas, with the Thole-type model potential (TTM3-F) [45] give for the dimer, trimer and tetramer, binding energies of −225, − 684 and −1163 meV, respectively, while our model potential, without no further refinement of the adopted value of the dipole moment of the water monomer and of the β parameter, predicts values of the binding energy for the dimer, trimer and tetramer, respectively equal to −228, −623 and −1137 meV. Moreover, the model also leads to an accurate prediction of the second virial coefficient for the dimer, which has been measured over a wide range of temperature (273–3000 K) [40,37](as is well known the virial coefficient is a very sensitive indicator of the strength, range and anisotropy of pair interactions).

3. The portability of AMPF to bulk water and ionic solutions

When extending the AMPF effective model potential to describe liquid water, the same values of the ε and R_0 parameters used to describe small water clusters were adopted. The only difference consisted in increasing the value of the dipole moment of the individual water monomer to 2.3 D (a value very similar to those used in most popular models for liquid water). This choice was validated by comparing some features of the systems considered,

computed by running MD simulations using the DL_POLY program package [46] for the NVE, NVT and NpT ensembles (with periodic boundary conditions), with experimental information. The electrostatic component of the interaction has been calculated using the Ewald sum [47], as typical for periodic (or pseudo-periodic) systems.

The bulk water analysis has been carried out by performing MD simulations for an NpT ensemble of 256 molecules of water subjected to the Berendsen thermostat and barostat [48].

The ionic solutions discussed below have been investigated by performing MD simulations for an NVE ensemble of 246 molecules of water and four alkali ions at a temperature of 300 K.

3.1. Bulk water

NpT molecular dynamics results, obtained at several values of the pressure, p, and the temperature, T, show that the calculated AMPF water density values are in reasonably good agreement with experimental data [37]. This is also the case of the mean configuration energy ranging from −445.9 meV at 273 K to −430.9 meV at 297 K [49]. The values of the self-diffusion coefficients for water at several temperatures have been also obtained, reproducing its increase with temperature. The calculated self-diffusion coefficients, as it has been found using other potential models to simulate liquid water [49], are higher than the experimental ones [50]. For instance, in Ref. [49] the self-diffusion coefficients obtained from the original SPC/E at $T = 298.6$ K (4.2×10^{-9} m^2 s^{-1}), the original TIP3P at 297 K (5.6×10^{-9} m^2 s^{-1}), the modified TIP3P at 299.2 K (5.9×10^{-9} m^2 s^{-1}) and the refined SPC at 297.7 K (4.2×10^{-9} m^2 s^{-1}) are reported and compared with the experimental value of 2.3×10^{-9} m^2 s^{-1} which corresponds to a temperature of about 298 K.

In the 274–298 K temperature range, the AMPF model predicts values of the self-diffusion coefficients ranging from 2.4×10^{-9} m^2 s^{-1} to 3.5×10^{-9} m^2 s^{-1}. This last value, higher than the experimental one is, however, lower than those predicted in Ref. [49] using other water potential models.

Radial distribution functions (g's) calculated on the AMPF model potential were also found to compare well with the neutron diffraction experimental data [16]. All the comparisons indicate that the AMPF model potential is well suited to describe the force field for water containing systems.

Though the mentioned results were obtained by adopting the same set of values of the V_{vdW} parameters used for small water clusters, one has to bear in mind that minor changes of β and/or of the monomer dipole moment values could further improve the agreement between calculated and experimental data. This is, indeed, what we did in some additional calculations. Related results obtained using slightly different values of the dipole moment of the water monomer are shown in Fig. 3, where the g functions calculated for a NpT ensemble are compared with the experimental results of Ref. [16]. The g_{OO} plots obtained for the water bulk using the AMPF model show three peaks in good agreement with those obtained, at the same temperature, from neutron diffraction experiments [16](represented as a continuous line in the figure). The same agreement is observed for the g_{OH} function (not reported in the figure).

3.2. From liquid water to solvated alkali ions: the M^+–H_2O systems (M = Li,Na,K,Rb,Cs)

Encouraged by the success obtained with the MD simulation of the water bulk, we have undertaken the study of the M^+–H_2O systems. This means that the interaction (including $V_{rep} + V_{ind} + V_{disp}$) was modeled in terms of a $V_{M^+\bar{O}}$ component and an electrostatic

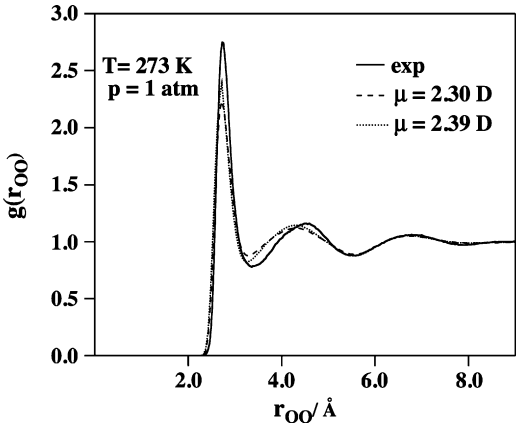

Fig. 3. g_{OO} plots calculated using two different dipole moment values (2.30 and 2.39 D, dashed and dotted lines, respectively) for the water monomer in the liquid compared with experimental data (solid line) taken at the same temperature.

one as follows:

$$V = V_{M^+\bar{O}} + V_{electr} \quad (6)$$

where the first term, $V_{M^+\bar{O}}$ (including $V_{vdW} + V_{ind}$), is formulated as in Eq. (5) by setting m equal to 4. The remaining parameters, calculated following the approach described in Refs. [23–25], are given in Table 3. Due to the fact that different ionic systems should have a different shape of the repulsive walls, specific β values were adopted for the various ions as pointed out also when constructing the PESs of other ionic clusters [27,51].

The second term, V_{electr}, is evaluated by taking into account the positive charge of the ion and a three-point charge distribution on the water molecule. It is important to mention here that the dipole moment of the H_2O monomer has been again considered only as an effective model parameter, related to the true dipole moment of H_2O in the ionic aggregate but not necessarily coincident with it. As a matter of fact, in our simulations the values 2.2, 2.1, 2.07, 2.05 and 2.0 D (for Li^+, Na^+, K^+, Rb^+ and Cs^+, respectively) have been used in order to best fit the information available for the interaction from literature [52–55].

Energy and intermolecular distance values predicted for the most stable geometry are given in Table 4 where corresponding experimental [52] and *ab initio* values [53,54] are also reported for comparison.

Table 3
Potential parameters of $V_{M^+\bar{O}}$ for the various M^+–H_2O systems

System	Li^+–H_2O	Na^+–H_2O	K^+–H_2O	Rb^+–H_2O	Cs^+–H_2O
ε (meV)	240.97	151.89	102.10	90.01	78.42
R_0 (Å)	2.386	2.732	3.161	3.335	3.546
β	4.5	6.0	7.0	7.4	8.0

Table 4
Minimum energy, V, and equilibrium $M^+\bar{O}$ distance, R, for the various M^+–H_2O aggregates calculated using the parameters given in Table 3 for $V_{M^+\bar{O}}$ and adding V_{electr} (see also the text)

System	Li^+–H_2O	Na^+–H_2O	K^+–H_2O	Rb^+–H_2O	Cs^+–H_2O	Reference
V (meV)	−1478	−1058	−777	−692	−610	Present
	−1477	−1041	−776	−689	−594	[52]
	−1374	−988	−771	−706	−619	[53]
	−1448	−1001	−776	...	...	[54]
R (Å)	2.042	2.372	2.760	2.935	3.129	Present
	1.879	2.292	2.669	...	...	[54]

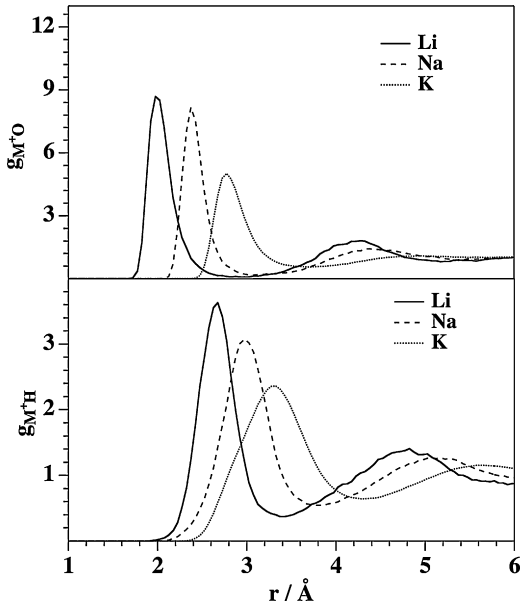

Fig. 4. Radial distribution functions for Li^+, Na^+ and K^+ in water with respect to O (upper panel) and H (lower panel).

The agreement appears to be satisfactory, confirming again the reliability of the formulation adopted for the model potential.

A final test was performed by calculating the *g*'s for solvated Li^+, Na^+ and K^+ ions by running DL_POLY [46] with $T = 300$ K and using, as already mentioned, an NVE ensemble of 246 water molecules with 4 ions ($[M]^+ \approx 0.9$ M). In the upper panel of Fig. 4 the calculated g's for solvated Li^+, Na^+ and K^+ with respect to the O atom (g_{M^+O}) are plotted.

The calculated first peaks of g_{Li^+O}, g_{Na^+O} and g_{K^+O} are located at 1.975, 2.375 and 2.775 Å, respectively. These values are in good agreement with the experimental data given in Ref. [54](1.96 Å for Li^+[56], 2.39 and 2.40 Å for Na^+[57,58] and 2.8 Å for K^+[59,60]). The predicted positions of the first peak also compare well with the results of Ref. [54] based on Car–Parrinello MD simulations using the density functional theory (1.99 Å for Li^+, 2.40 Å for Na^+ and 2.85 Å for K^+). In the lower panel of Fig. 4 the g's calculated for the same solvated ions with respect to the H atom ($g_{\{M\}+\{H\}}$) are shown. In this case too, a good agreement with results reported in the literature [54] is obtained.

Several simulations performed under different conditions confirmed that the energy of the most stable geometry (see Table 4) and the features of the g functions are strongly affected by the value of the β parameter which controls at the same time both the hardness of the repulsion and the dependence of the attraction on the intermolecular distance (see Eq. (5)).

4. Conclusions

In the present paper we illustrate the evolution of the formulation of a model potential (AMPF), linked to basic physical properties of the involved molecules, suited for being used in dynamical calculations thanks to its portability from monomeric species to bulk systems. The formulation of the potential allowed us to link the outcomes of an investigation of the rare gas–water monomer interaction with the dynamics of water clusters of increasing size (up to liquid bulks) and to propose an effective model potential to describe such interaction. The model showed to be also suitable to be extended to the description of ionic solutions. The validity of the proposed formulation was further confirmed (without performing any best fit) by comparing the description of the properties of the most stable geometry of neutral and ionic aggregates involving water. The AMPF model has been also used to predict the behaviour of the systems considered in other geometries and to carry out molecular dynamics simulations (performed using the DL_POLY suite of codes) whose outcomes were favourably compared with scattering and diffraction measurements. The most important characteristic analysed here concerns with the description of the van der Waals interaction by means of a simple but efficient functional form, useful to be used in MD simulations. As regards to electrostatic interaction, the value of 2.3 D for the monomer dipole moment has been used in the simulation of liquid water because of its similarity with that used by some of most popular models for water. As stressed above, in the AMPF model, most of the attention has focused onto an accurate description of van der Waals interaction more than on the electrostatic one. An interesting development of our study could be the combination of AMPF with different models of charge distributions (see for instance [61,62]) to analyse their effect on the predicted behaviour of liquid water.

Acknowledgments

M. Albertí and A. Aguilar acknowledge financial support from the Ministerio de Educación y Ciencia (Spain, Project CTQ2007-61109) and the Generalitat de Catalunya-DURSI (Project 2005 PEIR 0051/69). Also thanks are due to the Centre de Supercomputació de Catalunya CESCA-C4 and Fundació Catalana per a la Recerca for the allocated supercomputing time. D. Cappelletti, A. Laganà and F. Pirani acknowledge financial support from the Italian Ministry of University and Research (MIUR, PRIN 2005 Contracts No. 2004033958 and 2005033911_001).

References

[1] K. Morokuma, J. Chem. Phys. 55 (1971) 1236.
[2] K. Müller-Dethlefs, P. Hozba, Chem. Rev. 100 (2000) 143.
[3] http://www.lsbu.ac.uk/water/index.html.
[4] B. Guillot, J. Mol. Liq. 101 (2002) 219.
[5] J.L. Finney, J. Mol. Liq. 90 (2001) 303.
[6] R.S. Fellers, C. Leforestier, L.B. Braly, M.G. Brown, R.J. Saykally, Science 284 (1999) 945, and references therein.
[7] R.W. Bickes, G. Duquette, C.J.N. van den Meijdenberguer, A.M. Rulis, G. Scoles, K.M. Smith, J. Phys. B: At. Mol. Phys. 8 (1975) 3034.
[8] J.T. Slankas, M. Keil, A. Kuppermann, J. Chem. Phys. 79 (1979) 1482.
[9] J. Brudermann, C. Steinbech, U. Buck, K. Patkowski, R. Monszynzki, J. Chem. Phys. 117 (2002) 11166.
[10] D. Cappelletti, V. Aquilanti, E. Cornicchi, M. Moix Teixidor, F. Pirani, J. Chem. Phys. 123 (2005) 024302.
[11] V. Aquilanti, E. Cornicchi, M. Moix Teixidor, N. Saending, F. Pirani, D. Cappelletti, Angew. Chem. Int. Ed. 44 (2005) 2356.
[12] M.P. Hodges, R.J. Wheatley, A.H. Harvey, J. Chem. Phys. 116 (2002) 397.
[13] M.P. Hodges, R.J. Wheatley, A.H. Harvey, J. Chem. Phys. 117 (2002) 7169.
[14] J.C. Dore, M. Garawi, M.C. Bellissent-Funel, Mol. Phys. 102 (2004) 2015.
[15] F. Bruni, M.A. Ricci, A.K. Soper, J. Chem. Phys. 109 (1998) 1478.
[16] A.K. Soper, Chem. Phys. 258 (2000) 121.
[17] M. Albertí, A. Aguilar, J.M. Lucas, A. Laganà, F. Pirani, J. Phys. Chem. A 111 (2007) 1780.
[18] K.G. Denbigh, Trans. Faraday Soc. 36 (1940) 936.
[19] R.P. Smith, E.M. Mortensen, J. Chem. Phys. 32 (1960) 502.
[20] R. Cambi, D. Cappelletti, G. Liut, F. Pirani, J. Chem. Phys. 95 (1991) 1852.
[21] F. Huarte-Larrañaga, A. Aguilar, J.M. Lucas, M. Albertí, J. Phys. Chem. A 111 (2007) 8072.
[22] G. Liuti, F. Pirani, Chem. Phys. Lett. 122 (1985) 245.
[23] D. Cappelletti, G. Liuti, F. Pirani, Chem. Phys. Lett. 183 (1991) 297.
[24] V. Aquilanti, D. Cappelletti, F. Pirani, Chem. Phys. 209 (1996) 299.
[25] F. Pirani, G.S. Maciel, D. Cappelletti, V. Aquilanti, Int. Rev. Phys. Chem. 25 (2006) 165.
[26] F. Pirani, D. Cappelletti, G. Liuti, Chem. Phys. Lett. 350 (2001) 286.
[27] M. Albertí, A. Castro, A. Laganà, M. Moix, F. Pirani, D. Cappelletti, G. Liuti, J. Phys. Chem. A 109 (2005) 2906.
[28] F. Pirani, M. Albertí, A. Castro, M. Moix Teixidor, D. Cappelletti, Chem. Phys. Lett. 394 (2004) 37.
[29] F. Pirani, S. Brizi, L.F. Roncaratti, P. Casavecchia, D. Cappelletti, F. Vecchiocattivi, Phys. Chem. Chem. Phys. 10 (2008) 5489.
[30] A.D. Buckingham, Adv. Chem. Phys. 12 (1967) 133.

[31] M. Albertí, A. Castro, A. Laganà, F. Pirani, M. Porrini, D. Cappelletti, Chem. Phys. Lett. 392 (2004) 514.
[32] M. Albertí, A. Aguilar, J.M. Lucas, D. Cappelletti, A. Laganà, F. Pirani, Chem. Phys. 328 (2006) 221.
[33] M. Albertí, A. Castro, A. Laganà, M. Moix, F. Pirani, D. Cappelletti, Eur. Phys. J.D 38 (2006) 185.
[34] M. Albertí, A. Aguilar, A. Laganà, L. Pacifici, Chem. Phys. 327 (2006) 105.
[35] K. Patkowski, T. Korona, R. Moszinski, B. Jeziorski, K. Szalewicz, J. Mol. Struct. Theochem. 59 (2002) 231.
[36] G. Calderoni, F. Cargogni, M. Raimondi, Chem. Phys. Lett. 370 (2003) 233.
[37] M. Albertí, A. Aguilar, M. Bartolomei, D. Cappelletti, A. Laganà, J.M. Lucas, F. Pirani, Lect. Notes Comp. Sci. 5072 (2008) 1026.
[38] J.K. Gregory, D.C. Clary, K. Liu, M.G. Brown, R.J. Saykally, Science 275 (1997) 4705.
[39] K. Liu, M.G. Brown, R.J. Saykally, J. Phys. Chem. A 101 (1997) 8995.
[40] M. Albertí, A. Aguilar, M. Bartolomei, D. Cappelletti, A. Laganà, J.M. Lucas, F. Pirani, Physica Scripta 78 (2008) doi:10.1088/0031-8949/78/1/000000.
[41] R. Bukowsky, K. Szalewicz, G. Groenenboom, A. van der Avoird, J. Chem. Phys. 125 (2006) 044301.
[42] J.A. Anderson, K. Grager, L. Fedoroff, G.S. Tschumpe, J. Chem. Phys. 121 (2004) 11023.
[43] J.R. Reimers, R.O. Watts, M.L. Klein, Chem. Phys. 64 (1982) 65.
[44] S.S. Xantheas, C.J. Burnham, R.J. Harrison, J. Chem. Phys. 116 (2002) 1493.
[45] G.S. Fanourgakis, S.S. Xantheas, J. Chem. Phys. 128 (2008) 074506.
[46] http://www.cse.clrc.ac.uk/ccg/software/DL_POLY/index.shtml.
[47] M.P. Allen, D.J. Tildesley, Computer Simulation of Liquids, Clarendon Press, Oxford, 1989.
[48] H.J.C. Berendsen, J.P.M. Postma, W. van Gunsteren, A. DiNola, J.R. Haak, J. Chem. Phys. 81 (1984) 3684.
[49] P. Mark, L. Nilsson, J. Phys. Chem. A 105 (2001) 9954.
[50] R. Mills, J. Phys. Chem. 77 (1973) 685.
[51] M. Albertí, A. Aguilar, J.M. Lucas, F. Pirani, D. Cappelletti, C. Coletti, N. Re, J. Phys. Chem. A 110 (2006) 9002.
[52] P. Kebarle, Annu. Rev. Phys. Chem. 28 (1977) 445.
[53] J. Aqvist, J. Phys. Chem. 94 (1990) 8021.
[54] T. Ikeda, M. Boero, K. Terakura, J. Chem. Phys. 126 (2007) 034501.
[55] M.T. Rodgers, P.B. Armentrout, J. Chem. Phys. 101 (1997) 1238.
[56] Y. Kameda, O. Uemura, Bull. Chem. Soc. Jpn. 66 (1993) 384.
[57] N.T. Skipper, G.W. Neilson, J. Phys. Condens. Matter 1 (1989) 414.
[58] Y. Kameda, K. Sugawara, T. Usuki, O. Uemura, Bull. Chem. Soc. Jpn. 71 (1998) 2769.
[59] N. Ohtomo, K. Arakawa, Bull. Chem. Soc. Jpn. 53 (1980) 1789.
[60] G.W. Neilson, N.T. Skippe, Chem. Phys. Lett. 114 (1985) 35.
[61] S.W. Rick, S.J. Stuart, B.J. Berne, J. Chem. Phys. 101 (1994) 6141.
[62] P. Ren, J.W. Ponder, J. Phys. Chem. B 107 (2003) 5933.